

Shining a Light on Bose–Hubbard Mixtures

M. J. Bhaseen,¹ M. Hohenadler,^{1,2} A. O. Silver,¹ and B. D. Simons¹

¹*University of Cambridge, Cavendish Laboratory, Cambridge, CB3 0HE, UK.*

²*Present Address: OSRAM Opto Semiconductors GmbH, 93055 Regensburg, GER.*

(Dated: November 13, 2019)

Motivated by recent experiments on cold atomic gases in ultra high finesse optical cavities, we consider the problem of a two-band Bose–Hubbard model coupled to quantum light. Photoexcitation promotes carriers between the bands and we study the non-trivial interplay between Mott insulating behavior and superfluidity. The model displays a global $U(1) \times U(1)$ symmetry which supports the coexistence of Mott insulating and superfluid phases, and yields a rich phase diagram with multicritical points. This symmetry property is shared by several other problems of current experimental interest, including two-component Bose gases in optical lattices, and the bosonic BEC-BCS crossover problem for atom-molecule mixtures induced by a Feshbach resonance. We corroborate our findings by numerical simulations.

PACS numbers: 03.75.Mn, 03.75.Hh, 67.85.-d, 05.30.Jp

Introduction.— The spectacular advances in manipulating ultracold atomic gases have led to landmark experiments in strongly correlated systems. With the observation of the superfluid–Mott insulator transition in ⁸⁷Rb [1], and the BEC–BCS crossover in ⁴⁰K [2], significant attention is now being directed towards multicomponent gases. Whether they be distinct atoms or internal states of the same species, such systems bring additional “isospin” degrees of freedom. They offer the fascinating prospect to realize novel phases, and allow one to study the interplay between quantum magnetism, Mott insulating behavior and superfluidity [3, 4, 5].

More recently, significant experimental progress has been made in combining the tools of cavity quantum electrodynamics (cavity QED) with those of ultracold gases [6, 7, 8]. The realization of Bose–Einstein condensates in ultra high finesse optical cavities [6, 7, 8] opens up an exciting new chapter in coherent matter–light interaction. The cavity light field serves as both a probe of the many–body system, and may also support interesting cavity mediated phenomena and phases.

In this work we consider the impact of coherent cavity radiation on the Bose–Hubbard model. Specifically, we consider a two-band model in which cavity photons induce transitions between two internal states or Bloch bands. This may be regarded as a natural generalization of the much studied problems of two-level systems coupled to radiation, and may serve as a useful paradigm in other contexts. The important new ingredients are that the bosonic carriers may form a Mott insulator, or indeed condense. The primary question we are interested in is whether a novel Mott insulating state can survive, which supports a condensate of photoexcitations or mobile defects? In analogy with the problem of zero point fluctuations in Helium [9], this may be viewed as a form of supersolid in which fluctuations of the photon field induce defects. Whilst this question has its origin in the study of polariton condensates in fermionic band insula-

tors [10], the present problem is rather different. Since the integrity of the Mott state is intimately tied to the interactions, *a priori* it is far from clear that it survives the combined effects of itinerancy and photoexcitation. Nonetheless, the outcome of our analytical and numerical studies is affirmative, and the model displays both this novel phase and a rich phase diagram.

It is interesting to note that a related phase was very recently observed in Monte Carlo simulations of a simple two-component hardcore Bose–Hubbard model [11]. Although the problems are superficially rather different, the origins turn out to be similar and we will briefly discuss the connection to this work.

The Model.— Let us consider the problem of a two-band Bose–Hubbard model coupled to the coherent light field of an optical cavity as derived within the rotating wave approximation

$$H_0 = \sum_{i\alpha} \epsilon_\alpha n_i^\alpha + \sum_{i\alpha} \frac{U_\alpha}{2} n_i^\alpha (n_i^\alpha - 1) + V \sum_i n_i^a n_i^b - \sum_{\langle ij \rangle \alpha} J_\alpha \alpha_i^\dagger \alpha_j + \omega \psi^\dagger \psi + g \sum_i \left(b_i^\dagger a_i \psi + \text{h.c.} \right), \quad (1)$$

where $\alpha = a, b$ are two bands of bosonic carriers with canonical commutation relations $[\alpha_i, \alpha_j^\dagger] = \delta_{ij}$. These might be states of different orbital or spin angular momentum. Here, ϵ_α , are on–site potentials effecting the band splitting, U_α and V are on–site interactions, J_α , are nearest–neighbor hopping parameters, and ω is the frequency of the cavity mode, ψ . For simplicity we consider just a single cavity mode, which couples uniformly to the two bands. The coupling g describes the strength of the matter–light interaction, and in view of the box normalization of the photon field, it is convenient to denote $g \equiv \bar{g}/\sqrt{N}$, where N is the number of lattice sites. It is readily seen that $N_1 = \sum_i (n_i^b + n_i^a)$ and $N_2 = \psi^\dagger \psi + \sum_i (n_i^b - n_i^a + 1)/2$, commute with the Hamiltonian. These represent the total number of

atomic carriers, and the total number of photoexcitations (or polaritons) respectively. These conservation laws are a direct reflection of the global $U(1) \times U(1)$ symmetry of the Hamiltonian (1), such that $a \rightarrow e^{i\vartheta}a$, $b \rightarrow e^{i\varphi}b$, $\psi \rightarrow e^{-i(\vartheta-\varphi)}\psi$, where ϑ, φ are arbitrary real numbers. This symmetry will have a direct manifestation in the overall phase diagram, and suggest implications for other multicomponent problems. For simplicity, we begin by assuming that the a -particles are strongly interacting hardcore bosons (so that their occupancy is limited to zero or one) and that the b -particles are sufficiently dilute that we may neglect their interactions. We will consider their effects in the subsequent variational analysis below.

Zero Hopping Limit.— In order to gain insight into the model (1) it is convenient to examine the zero hopping limit. This will anchor the phase diagram to an exactly solvable many body limit, and also expose methods that generalize. In particular, the global photon mode couples to all sites and, in the thermodynamic limit it may be described by a coherent state, $|\gamma\rangle \equiv e^{-\frac{\gamma^2}{2}} e^{\gamma\psi^\dagger}|0\rangle$, with mean occupation $\langle\psi^\dagger\psi\rangle = \gamma^2$. We may thus replace the grand canonical Hamiltonian, $H \equiv H_0 - \mu_1 N_1 - \mu_2 N_2$, by an effective single site problem, $\langle\gamma|H|\gamma\rangle \equiv \sum_i \mathcal{H}_i$, where

$$\mathcal{H} \equiv \sum_{\alpha} \tilde{\epsilon}_{\alpha} n_{\alpha} + \tilde{\omega} \bar{\gamma}^2 + \bar{g} \bar{\gamma} (b^\dagger a + a^\dagger b), \quad (2)$$

and we drop the offset, $-\mu_2/2$. Here we absorb the chemical potentials in to the coefficients $\tilde{\epsilon}_a \equiv \epsilon_a - \mu_1 + \mu_2/2$, $\tilde{\epsilon}_b \equiv \epsilon_b - \mu_1 - \mu_2/2$, $\tilde{\omega} \equiv \omega - \mu_2$. We also denote the mean photon occupation per site, $\bar{\gamma}^2 \equiv \gamma^2/N$. The effective Hamiltonian (2) describes a single two-level system coupled to an effective “radiation field” of b -particles, or the Jaynes–Cummings model [12, 13]; for N two-level systems this is known as the Dicke [14] or Tavis–Cummings model [15] and is integrable [16, 17, 18]. These paradigmatic models are well known in both atomic physics and quantum optics, and also emerge in problems of localized excitons coupled to light [19]. More recently, such systems have been realised in pioneering solid state cavity QED experiments [20, 21, 22]. For our purposes it is sufficient to note that (2) is readily diagonalized in terms of eigenstates that are superpositions of particles in the upper and lower bands (that we may denote as $|0, n\rangle$ and $|1, n-1\rangle$) with total occupancy n ; see for example Ref. 23. The lowest superposition has energy

$$E_n^- = \tilde{\omega} \bar{\gamma}^2 + n \tilde{\epsilon}_b - \tilde{\omega}_0/2 - \sqrt{\tilde{\omega}_0^2/4 + \bar{g}^2 \bar{\gamma}^2 n}, \quad (3)$$

where $\tilde{\omega}_0 \equiv \tilde{\epsilon}_b - \tilde{\epsilon}_a$. Minimizing with respect to $\bar{\gamma}$ gives a variational self-consistency equation for the photon field, and the resulting eigenstates yield the zero hopping phase diagram depicted in Fig. 1. In the thermodynamic limit described here, it turns out that only the lowest Mott state, with $n_a + n_b = 1$, survives; for $\mu_1 \geq \epsilon_b - \mu_2/2 - \bar{g}^2/4\tilde{\omega}$ it is energetically favorable

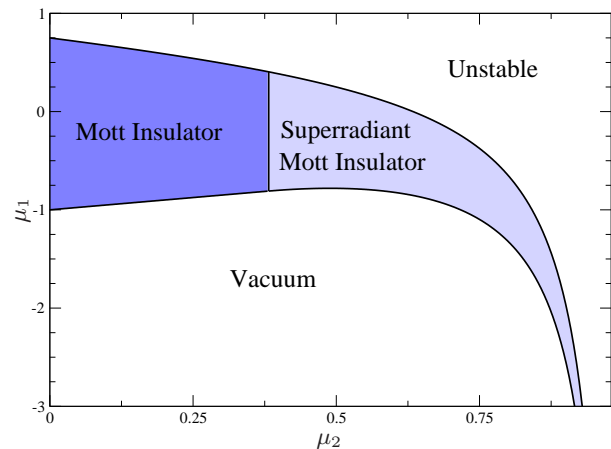


FIG. 1: Zero hopping phase diagram in the large- U_a limit, with $\epsilon^{(b)} = -\epsilon^{(a)} = \omega = \bar{g} = 1$, corresponding to $\omega < \omega_0$. The vertical line, $\bar{g} = \bar{g}_c$, is the superradiance transition in the Dicke model, and separates a Mott insulator with $n_a + n_b = 1$ and $\langle\psi^\dagger\psi\rangle = 0$ (dark blue), from a superradiant Mott insulator with $\langle\psi^\dagger\psi\rangle \neq 0$ (light blue). Outside of these regions are the vacuum state, and an unstable region corresponding to macroscopic population of the b states. Whilst the total density is fixed within both Mott phases, the individual a and b populations vary in the superradiant phase and may be viewed in terms of isospin order. For $\omega > \omega_0$, the upper and lower boundaries may cross and terminate the Mott lobe.

to macroscopically populate the upper band. Within this stable Mott phase the variational equation yields either $\bar{\gamma} = 0$, corresponding to zero photon occupancy, or $\bar{\gamma}^2 = (\bar{g}^4 - \bar{g}_c^4)/4\tilde{\omega}^2\bar{g}^2$, where $\bar{g}_c \equiv \sqrt{\tilde{\omega}\tilde{\omega}_0}$; the former occurs for $\bar{g} \leq \bar{g}_c$ and the latter for $\bar{g} \geq \bar{g}_c$. In fact, this onset corresponds to the superradiance transition in the Dicke model [14, 16, 17, 18]; see for example Table 1 of Ref. 24. Indeed, since $n_a + n_b = 1 \equiv 2S$ in the lowest lobe, one may construct the Dicke model directly from (1) by using a spin $S = 1/2$ Schwinger boson representation for $su(2)$, where $S^+ \equiv b^\dagger a$, $S^- \equiv a^\dagger b$, $S^z \equiv (n_b - n_a)/2$ [25]:

$$H = \tilde{\omega}_0 \sum_i S_i^z + \tilde{\omega} \psi^\dagger \psi + g \sum_i \left(S_i^\dagger \psi + \text{h.c.} \right). \quad (4)$$

This describes N two-level systems (or spins) coupled to a global photon mode, and may be treated using *collective* spin operators, $\mathbf{J} \equiv \sum_i^N \mathbf{S}_i$. This yields a large effective spin, and a semiclassical analysis becomes exact in the thermodynamic limit, $N \rightarrow \infty$. The onset of the photon field is naturally accompanied by a non-vanishing magnetization, $\mathcal{M} \equiv \langle J^z \rangle / N$, which also serves as an order parameter for this continuous transition: $\mathcal{M} = -1/2$, for $\bar{g} \leq \bar{g}_c$, and $\mathcal{M} = -(\bar{g}_c/\bar{g})^2/2$, for $\bar{g} \geq \bar{g}_c$. This growth reflects the relative population imbalance, $\langle n_b \rangle - \langle n_a \rangle$, due to the addition of photoexcitations. The agreement between the variational analysis based on a coherent state for ψ , and the exact Dicke model results is clearly a useful anchor point for our subsequent departures.

Variational Phase Diagram.— Having established the existence of a zero hopping Mott phase, with pinned integer density, $n_a + n_b = 1$, let us now consider the effects of itinerancy and carrier superfluidity. In the light of our previous discussion, we only need work within the lowest lobe, and may therefore work with hardcore a and b bosons [38]. A convenient and intuitive way to proceed is to augment the real space variational approach of Altman *et al* [4] with a coherent state for the light field. We take as our variational state

$$|\mathcal{V}\rangle = \prod_i \left[\cos \theta_i (\cos \chi_i a_i^\dagger + \sin \chi_i b_i^\dagger) + \sin \theta_i (\cos \eta_i + \sin \eta_i b_i^\dagger a_i^\dagger) \right] |\gamma\rangle, \quad (5)$$

where $|\gamma\rangle$ is the coherent state introduced previously, and we subsume the local a, b vacua into the definition of $|0\rangle$. Here, $\theta, \chi, \eta, \gamma$ are variational parameters to be determined. The first term in brackets describes the Mott insulator, and the second allows for superfluidity. For $\theta = 0$ this coincides with the variational approach used to describe localized excitons coupled to light [10] and reproduces the previous results for $J_\alpha = 0$. More generally, the variational state (5) takes into account the effects of *real* hopping processes, involving genuine site vacancies and interspecies double occupation. As such, it provides a useful starting point to identify the boundaries between the Mott insulating and superfluid regions. For simplicity we consider only spatially homogeneous phases and take the variational parameters to be site independent. For the Hamiltonian (1) this gives rise to the variational energy per site, $\mathcal{E} \equiv \langle \mathcal{V} | H | \mathcal{V} \rangle / N$:

$$\begin{aligned} \mathcal{E} &= (\tilde{\epsilon}_+ - \tilde{\epsilon}_- \cos 2\chi) \cos^2 \theta + (2\tilde{\epsilon}_+ + V) \sin^2 \eta \sin^2 \theta \\ &\quad - \frac{z}{4} [J_a \cos^2(\chi - \eta) + J_b \sin^2(\chi + \eta)] \sin^2 2\theta \\ &\quad + \tilde{\omega} \tilde{\gamma}^2 + \bar{g} \tilde{\gamma} \cos^2 \theta \sin 2\chi, \end{aligned} \quad (6)$$

where z is the lattice coordination number and $\tilde{\epsilon}_\pm \equiv (\tilde{\epsilon}_b \pm \tilde{\epsilon}_a)/2$. Minimizing with respect to $\tilde{\gamma}$ yields $\tilde{\gamma} = -\bar{g} \cos^2 \theta \sin 2\chi / 2\tilde{\omega}$, and one may eliminate this variable from the variational energy. Exploiting translation symmetry through π , inversion symmetry, and the locking of the signs of η and χ , one may minimize this function over the intervals $[0, \pi/2]$. Using the expressions for the order parameters, $\langle a \rangle = \frac{1}{2} \sin 2\theta \cos(\chi - \eta)$, and $\langle b \rangle = \frac{1}{2} \sin 2\theta \sin(\chi + \eta)$, and the fact that $\langle \psi^\dagger \psi \rangle / N = \tilde{\gamma}^2$, this translates in to the generic phase diagram depicted in Fig. 2, where we set $J_a = J_b = J$. For the chosen parameters, we have four distinct phases. These are (i) a Mott insulator with $\langle a \rangle = \langle b \rangle = \langle \psi^\dagger \psi \rangle = 0$, (ii) a superradiant Mott insulator with $\langle a \rangle = \langle b \rangle = 0$ and $\langle \psi^\dagger \psi \rangle \neq 0$, (iii) a single component superfluid with $\langle a \rangle \neq 0$ and $\langle b \rangle = \langle \psi^\dagger \psi \rangle = 0$, and (iv) a superradiant superfluid $\langle a \rangle \neq 0$, $\langle b \rangle \neq 0$, $\langle \psi^\dagger \psi \rangle \neq 0$. A simple way to understand this is that the Hamiltonian displays a

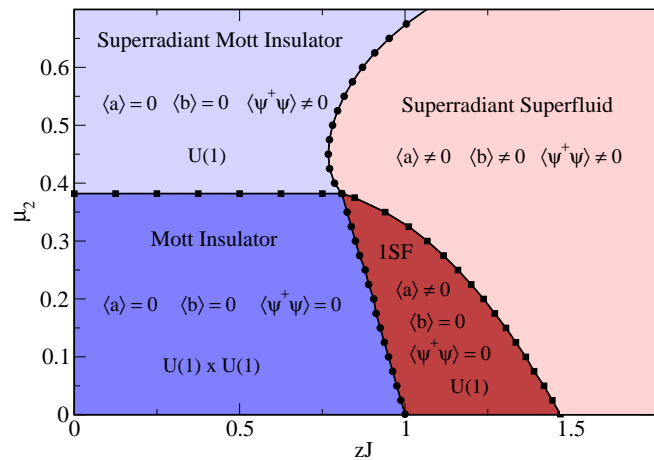


FIG. 2: Variational phase diagram in the μ_2 versus zJ plane, with $J_a = J_b = J$ and $\epsilon_a = -1$, $\epsilon_b = 1$, $\omega = 1$, $V = 1$, $\bar{g} = 1$, $\mu_1 = 0$. The phases are (i) a Mott insulator with $\langle \psi^\dagger \psi \rangle = 0$ (dark blue), (ii) a superradiant Mott insulator with $\langle \psi^\dagger \psi \rangle \neq 0$, and supporting a condensate of photoexcitations (light blue), (iii) a superradiant superfluid with $\langle \psi^\dagger \psi \rangle \neq 0$ (light red), and (iv) a one component a -type superfluid with $\langle \psi^\dagger \psi \rangle = 0$ (dark red). The circles denote the transition to superfluidity as determined by the onset of θ , and the squares denote the onset of photon number as determined by the admixture parameter χ . For these parameters, the transition from the Mott insulator to the superradiant Mott insulator occurs for $\mu_2^c = (3 - \sqrt{5})/2 \approx 0.382$.

$U(1) \times U(1)$ symmetry and these may be broken independently. The variational phase diagram therefore reflects the natural pattern of symmetry breaking allowed by the Hamiltonian (1). In particular the superradiant Mott insulator corresponds to an unbroken $U(1)$ in the matter sector (corresponding to a pinned number density and large phase fluctuations) but a broken $U(1)$ (or phase coherent condensate) in the photoexcitation sector. This novel phase may thus be regarded as a form of supersolid.

In the absence of competition from other phases, the transition between the non-superradiant Mott insulator ($\theta = \chi = \tilde{\gamma} = 0$) and the one component a -type superfluid ($\theta \neq 0$, $\chi = \eta = \tilde{\gamma} = 0$) occurs when $\tilde{\epsilon}_a + zJ = 0$. For the parameters used in Fig. 2, this is the straight line $\mu_2 = 2(1 - zJ)$. The intersection with the J independent superradiance boundary yields a tetracritical point at $(zJ^c, \mu_2^c) = (r/2, 2 - r)$, where $r \equiv (1 + \sqrt{5})/2$ is the Golden ratio. This also follows from a Landau expansion of the variational energy (6); after eliminating $\tilde{\gamma}$, all the quadratic “mass” terms involving θ , χ , and η vanish at this point and yield, $\mathcal{E} = -r/2 + \mathcal{O}(4)$. More generally, the overall phase diagram evolves with the system parameters, and the a -type superfluid may be eliminated in favor of the proximate phases, for example [26].

Numerical Simulations.— In order to corroborate our analytical results, we present exact diagonalization results for a one-dimensional system of hardcore a and b

bosons, with $N = 8$ sites and periodic boundary conditions. The Hilbert space is truncated by imposing a maximum number of photons, M_ψ [39]. Here we take $M_\psi = 2N = 16$. The effects of this truncation, as well as system size, will be discussed in detail in Ref. 26.

Once the ground state has been obtained numerically, physical observables of interest can be calculated. Fig. 3 shows results for the total atom, photon, a -atom and b -atom density. The dashed lines indicate the approximate locations of the Mott insulator–superfluid (vertical line) and superradiance (horizontal line) transitions, as determined from panels (a) and (b). Although an accurate phase diagram for the thermodynamic limit is beyond the scope of the present work, the overall features are in excellent agreement with the phase diagram depicted in Fig. 2. This parallels the qualitative success of mean field theory in other low-dimensional bosonic systems, and is quite remarkable given the enhanced role of fluctuations in one dimension. In the present case this success may also be attributed to the long range interactions induced by the global photon field.

The principal features to note are that the superradiance transition encompasses both the superfluid and Mott insulating phases, and yields a tetracritical point; see panels (a) and (b). In addition, the region of a -atom density over–extends that of b -atom density resulting in a single component a -type superfluid; see panels (c) and (d). Our current numerical simulations suggest that this phase is stable with respect to increasing system size [26].

Discussion.— Having presented both analytical and numerical results in favor of the predicted phase diagram, let us reflect on our findings and develop a broader picture. A feature not addressed by the present mean field theory, but captured in Fig. 3, is the dispersion of the superradiance transition with J ; in the Mott phase, $\theta = 0$, and J drops out of the variational energy (6). One way to understand this is to recast the matter contribution to the variational wavefunction in the form

$$|\mathcal{V}_M\rangle = \prod_i \left[\cos \chi_i + \sin \chi_i b_i^\dagger a_i \right] |\Omega\rangle, \quad (7)$$

where we effect a change of reference vacuum to the filled Mott state $|\Omega\rangle \equiv \prod_i a_i^\dagger |0\rangle$. It is readily seen that the variational state (7) only accomodates *local* particle-hole pairs on top of the filled Mott background. The variational ansatz neglects the *virtual* hopping processes [4] that allow the particle-hole pairs to spread out and to maximize their kinetic energy. In analogy with the BCS approach to the exciton insulator [27, 28], one anticipates that the detailed structure of the Mott state may be refined by a momentum space pairing wavefunction [26].

This connection to the BEC–BCS crossover problem for bosons [29] may be further reinforced by analogy with the bosonic Feshbach resonance problems studied in the absence of an optical lattice [30, 31, 32]. Performing a particle–hole transformation, the matter–light coupling

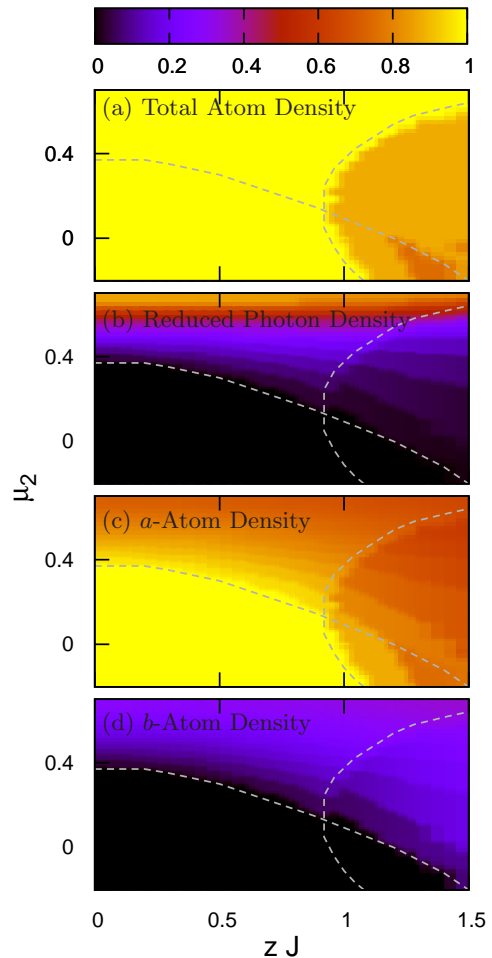


FIG. 3: Exact diagonalization results for a one-dimensional system with $N = 8$ sites and $M_\psi = 16$ photons (see text) and the same parameters as in Fig. 2. The panels show (a) the total atom density and the associated Mott insulator to superfluid transition, (b) the density of photons (reduced by a factor of two) indicating the onset of superradiance, (c) the density of a -atoms, and (d) the density of b -atoms. The dashed lines are intended solely as a guide to the eye, and indicate the approximate locations of the Mott insulator–superfluid and superradiance transitions; they are determined by hand from panels (a) and (b). Their intersection yields the location of the tetracritical point within this finite size simulation.

takes the form $\psi^\dagger a_i b_i$. Aside from the global nature of the photon field, this describes the conversion of a and b particles into a “molecule” ψ . At the outset there are eight possible phases corresponding to the separate condensation of the expectation values $\langle a \rangle$, $\langle b \rangle$, $\langle \psi \rangle$. Of these, only five phases may survive; condensation of two variables provides an effective field (as dictated by the coupling) which induces condensation of the other. In breaking the symmetry between the bands, $\epsilon_a < \epsilon_b$, this

is further reduced to four, or in general less, depending on the parameters. In contrast to the single species Feshbach resonance problem, the two-species case supports an additional atomic superfluid, since condensation of one of the carriers no longer induces an effective field. Moreover, condensation of one of the variables leaves a residual U(1) symmetry intact, which allows the non-trivial interplay between Mott insulating and phase coherent behavior.

Note that in deriving our variational energy (6) and the associated phase diagram, we are primarily concerned with the interesting effects of the matter-light coupling. As such, we incorporate V in the same way as in Ref. 4. This approach gives rise to the additional non-trivial phases shown in Fig. 2. However, as recently noted by Söyler *et al* [11], analogous phases may also be stabilized in the simple two-component Bose–Hubbard model, *without* explicit matter-light coupling, through a more sophisticated treatment of V itself. Indeed, on-site repulsive interactions, $Vn_a n_b$, favor a particle of one species and a hole of the other on the same site. Treating this “particle-hole pairing” in a BCS like mean field approach, one may replace the quartic interaction, $n_i^a n_i^b$, by $|\Delta_i|^2 + (\Delta_i b_i^\dagger a_i + \text{h.c.})$, where the pairing order parameter, $\Delta_i \equiv \langle a_i^\dagger b_i \rangle$, is to be determined self-consistently. As such, the decoupling field plays a similar role to a *local* photon field, and a similar phenomenology may ensue at the mean field level. Such pairing also occurs in the analogous fermionic two-band Hubbard model [33, 34]. Although, the majority of our discussion has focused on a single *global* photon field, the symmetry analysis of the condensation scenarios is more general. This is supported by studies of the two-band Bose–Hubbard model for equal fillings and commensurate densities [35]. We shall provide details of the similarities and differences of this site local problem in Ref. 26. The classical limit may also be realized in optical superlattices [36], where $g_i a_i b_i^\dagger$ represents tunnelling between different wells, a and b .

Conclusions.— In this work we have considered the impact of photoexcitations on the Bose–Hubbard model. The zero temperature phase diagram supports a novel phase where photoexcitations condense on the background of a Mott insulator. We have supplemented these findings by numerical simulations, and highlighted connections to other problems of current interest. The matter–light system provides physical intuition and a useful framework, and fosters links between different communities. There are many directions for further research. These include the impact of fluctuations on the variational phase diagram, and the nature of collective excitations. It would also be interesting to perform more detailed studies incorporating a finite photon wavevector. This may stabilize inhomogeneous phases and provide a useful probe of incommensurate magnetism. Numerical simulations and a study of the two-component Feshbach resonance problem for bosons are currently in prepara-

tion [26]. In the light of our findings it would be instructive to investigate the thermodynamic order of the transitions in Ref. 11 in more detail. It is also interesting to note that very recent studies of Bose–*Fermi* mixtures in optical lattices display a similar phenomenology, in which superfluidity is replaced by fermionic metallicity [37].

Acknowledgements.— We thank G. Conduit, N. Cooper and M. Köhl for valuable discussions, and M. Rutter for helpful computing advice. We are especially grateful to J. Keeling for numerous suggestions and illuminating discussions of the recent literature. MJB, AOS, and BDS acknowledge funding under EPSRC grant no. EP/E018130/1. MH was supported by the FWF Schrödinger Fellowship No. J2583.

-
- [1] M. Greiner, O. Mandel, T. Esslinger, T. W. Hänsch, and I. Bloch, *Nature* **415**, 39 (2002).
 - [2] C. A. Regal, M. Greiner, and D. S. Jin, *Phys. Rev. Lett.* **92**, 040403 (2004).
 - [3] L. M. Duan, E. Demler, and M. D. Lukin, *Phys. Rev. Lett.* **91**, 090402 (2003).
 - [4] E. Altman, W. Hofstetter, E. Demler, and M. D. Lukin, *New J. Phys.* **5**, 113 (2003).
 - [5] M. Rodríguez, S. R. Clark, and D. Jaksch, *Phys. Rev. A* **77**, 043613 (2008).
 - [6] F. Brennecke, T. Donner, S. Ritter, T. Bourdel, M. Köhl, and T. Esslinger, *Nature* **450**, 268 (2007).
 - [7] F. Brennecke, S. Ritter, T. Donner, and T. Esslinger, *Science* **322**, 235 (2008).
 - [8] S. Ritter, F. Brennecke, C. Guerlin, K. Baumann, T. Donner, and T. Esslinger, [arXiv:0811.3967](https://arxiv.org/abs/0811.3967).
 - [9] A. F. Andreev and I. M. Lifshitz, *Sov. Phys. JETP* **29**, 1107 (1969).
 - [10] P. B. Littlewood, P. R. Eastham, J. M. J. Keeling, F. M. Marchetti, B. D. Simons, and M. H. Szymanska, *J. Phys. Cond. Matt* **16**, S3597 (2004).
 - [11] S. G. Söyler, B. Capogrosso-Sansone, N. V. Prokof'ev, and B. V. Svistunov, [arXiv:0811.0397](https://arxiv.org/abs/0811.0397).
 - [12] E. T. Jaynes and F. W. Cummings, *Proc. IEEE* **51**, 89 (1963).
 - [13] F. W. Cummings, *Phys. Rev.* **140**, A1051 (1965).
 - [14] R. H. Dicke, *Phys. Rev.* **93**, 99 (1954).
 - [15] M. Tavis and F. W. Cummings, *Phys. Rev.* **170**, 379 (1968).
 - [16] K. Hepp and E. H. Lieb, *Annals of Physics* **76**, 360 (1973).
 - [17] K. Hepp and E. H. Lieb, *Phys. Rev. A* **8**, 2517 (1973).
 - [18] Y. K. Wang and F. T. Hioe, *Phys. Rev. A* **7**, 831 (1973).
 - [19] P. R. Eastham and P. B. Littlewood, *Solid State Comm.* **116**, 357 (2000).
 - [20] A. Wallraff, D. I. Schuster, A. Blais, L. Frunzio, R.-S. Huang, J. Majer, S. Kumar, S. M. Girvin, and R. J. Schoelkopf, *Nature* **431**, 162 (2004).
 - [21] M. Hofheinz, E. M. Weig, M. Ansmann, R. C. Bialczak, E. Lucero, M. Neeley, A. D. O'Connell, H. Wang, J. M. Martinis, and A. N. Cleland, *Nature* **454**, 310 (2008).
 - [22] J. M. Fink, M. Göppl, M. Baur, R. Bianchetti, P. J. Leek, A. Blais, and A. Wallraff, *Nature* **454**, 315 (2008).

- [23] A. D. Greentree, C. Tahan, J. H. Cole, and L. C. L. Hollenberg, *Nature Physics* **2**, 856 (2006).
- [24] C. Emary and T. Brandes, *Phys. Rev. E* **67**, 066203 (2003).
- [25] A. Auerbach, *Interacting Electrons and Quantum Magnetism* (Springer, 1994).
- [26] M. J. Bhaseen, M. Hohenadler, A. O. Silver, and B. D. Simons, in preparation.
- [27] L. V. Keldysh and Y. V. Kopaeve, *Sov. Phys. Solid State* **6**, 2219 (1965).
- [28] L. V. Keldysh and A. N. Kozlov, *Sov. Phys. JETP* **27**, 521 (1968).
- [29] A. Koetsier, P. Massignan, R. A. Duine, and H. T. C. Stoof, [arXiv:0809.4189](https://arxiv.org/abs/0809.4189).
- [30] L. Radzihovsky, J. Park, and P. B. Weichman, *Phys. Rev. Lett.* **92**, 160402 (2004).
- [31] M. W. J. Romans, R. A. Duine, S. Sachdev, and H. T. C. Stoof, *Phys. Rev. Lett.* **93**, 020405 (2004).
- [32] L. Zhou, J. Qian, H. Pu, W. Zhang, and H. Y. Ling, *Phys. Rev. A* **78**, 053612 (2008).
- [33] K. Winkler, G. Thalhammer, F. Lang, R. Grimm, J. H. Denschlag, A. J. Daley, A. Kantian, H. P. Büchler, and P. Zoller, *Nature* **441**, 853 (2006).
- [34] A. Kantian, A. J. Daley, P. Törmä, and P. Zoller, *New J. Phys.* **9**, 407 (2007).
- [35] A. Kuklov, N. Prokof'ev, and B. Svistunov, *Phys. Rev. Lett.* **92**, 050402 (2004).
- [36] A. M. Rey, V. Gritsev, I. Bloch, E. Demler, and M. D. Lukin, *Phys. Rev. Lett.* **99**, 140601 (2007).
- [37] S. Sinha and K. Sengupta, [arXiv0811.4515](https://arxiv.org/abs/0811.4515).
- [38] Whilst this does not affect the physics *within* the lobe, where $n_a + n_b = 1$, the form of the upper boundary is modified by the permissible b population.
- [39] We consider the basis of tensor product states $|\phi^{(\nu)}\rangle = |\phi_a^{(\nu)}\rangle \otimes |\phi_b^{(\nu)}\rangle \otimes |\phi_\psi^{(\nu)}\rangle$, where $\nu = 1, \dots, M$. The atomic basis states are $|\phi_\alpha^{(\nu)}\rangle = |n_1^\alpha, n_2^\alpha, \dots, n_N^\alpha\rangle^{(\nu)}$, where $n_i^\alpha = 0, 1$ for hardcore bosons, and the photon basis states are of the form $|n_\psi\rangle$, where $n_\psi = 0, 1, \dots, M_\psi$. The total matrix dimension is $M = 2^N 2^N M_\psi$, and is equal to about 1E6 for the results of Fig. 3.